J Mater Sci (2011) 46:6904–6909
DOI 10.1007/s10853-011-5655-9

Torsion of semi-auxetic rods

Teik-Cheng Lim

Received: 18 March 2011 / Accepted: 24 May 2011 / Published online: 4 June 2011

Abstract A method for quantifying the overall Poisson's ratio of a rod undergoing torsional loading is proposed and applied for a concentrically compound rod with inner core and outer shell of similar shape but opposite Poisson's ratio signs. Results show that a concentric compound rod with auxetic core exhibit same effective Poisson's ratio signs but with greater magnitude under torsional loading than under axial loading. However, a concentric compound rod with auxetic shell exhibits a range of volume fraction whereby the overall auxeticity of the rod is loading mode dependent, i.e., it behaves as a conventional rod under axial loading but as an auxetic rod under torsional loading. Hence a compound rod with conventional core and auxetic shell can be used as a smart structure that gives different response depending on the type of loading imposed on it.

Introduction

As in the case of negative thermal expansion materials (e.g., [1–3]) and negative refractive index materials (e.g., [4]), negative Poisson's ratio materials, which are also known as auxetic materials, possess material behavior that is counter intuitive. Most materials exhibit positive Poisson's ratio, in that they get thinner or fatter when stretched or compressed, respectively. Auxetic materials are solids that behave in the opposite way. Due to the counter intuitive manner by which they behave, investigations into auxetic materials have been pioneered [5–12]. Numerous models have been proposed to shed insights for elucidating the negative Poisson's ratio behavior and its other accompanying properties (e.g., [13–18]). Equally explored is the interdisciplinary area of auxetic composites [19–22], whereby methods for processing auxetic fiber composites have been established (e.g., [23, 24]) and the behavior of auxetic fibers in composites have been investigated [25–27]. Depending on the stacking sequence of conventional anisotropic laminas, auxetic behavior has been found in the in-plane or out-of-plane of laminates. As a subset of this, a laminate made from isotropic laminas with alternating conventional and auxetic laminas exhibits Young's modulus that not only exceeds the simple rule of mixture but also exceeds the modulus of the stiffer phase [28–33]. A similar effect is seen in the use of fibers and matrix materials of different Poisson's ratio signs [34]. An example of the above-mentioned laminate is that of bimaterial strip that consists of significantly different property, such as their Poisson's ratios [35, 36]. Another example is the sandwich structure with auxetic cores or auxetic facesheets [37–45]. In view of the recent work on auxetic cylinders, tubes, rods and related geometry [46–48], this article proposes a way to evaluate the effective Poisson's ratio of a rod consisting of a core and shell of similar shape but possessing opposite Poisson's ratio signs.

Theory and formulation

Consider a rod of length L made from N number of discs in a series arrangement as shown in Fig. 1a, and another rod also of length L made from N number of hollow rods of similar shape in concentric arrangement as shown in Fig. 1b.

With reference to Fig. 1a, a rod consisting of different material properties arranged in series will experience

T.-C. Lim (✉)
School of Science and Technology, SIM University (UniSIM), Singapore, Singapore
e-mail: alan_tc_lim@yahoo.com

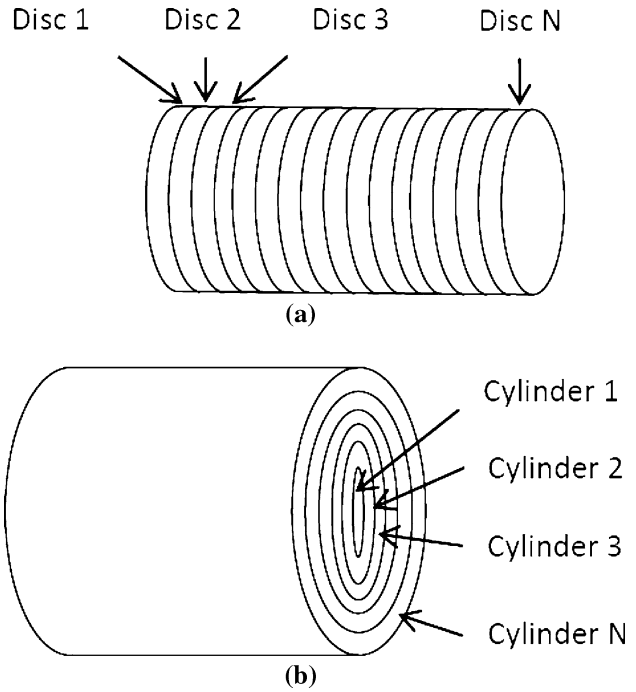

Fig. 1 A rod made from N different materials in **a** series arrangement, and **b** concentric arrangement

common torsion while the twist angle distribution is piecewise. Therefore, a single or constant torque is imposed

$$T = T_n; \quad (n = 1, 2, \ldots, N) \tag{1}$$

while the overall angular twist over the entire length of the rod is summed up from individual twist angles from every disc, i.e.,

$$\varphi = \sum_{n=1}^{N} \varphi_n. \tag{2}$$

Conversely, the torsion of a rod made from concentrically similar-shaped rods, as shown in Fig. 1b, produces common angular twist from one end to the other, while the torsional load is piecewise distributed radially. Therefore, a single or constant angular twist is imposed

$$\varphi = \varphi_n; \quad (n = 1, 2, \ldots, N) \tag{3}$$

while the total torsional load is summed from individual torsional load from each concentric rod.

$$T = \sum_{n=1}^{N} T_n. \tag{4}$$

The framework specified by Eqs. 3 and 4 is adopted in the proceeding analysis. It follows that this model is valid for perfect bonding at the interfaces of adjacent cylinders, and that the elastic properties from the bonding adhesive is negligible if it's modulus is in the same order as those of the concentric cylinders with the adhesive thickness being very small in comparison to the radial dimension of each cylinder. The relation between the applied torsion, rod length, shear modulus, polar moment area perpendicular to the torsional axis, and the angular twist for a solid prismatic rod of arbitrary cross-section is given by

$$\frac{TL}{\varphi} = GJ = GCD^4 \tag{5}$$

whereby the polar moment area of the solid rod's cross-section is $J = CD^4$, in which D is a characteristic dimension of the rod cross-section and C is cross-sectional shape dependent coefficient. Writing

$$G = \frac{E}{2(1+v)}, \tag{6}$$

we have the following relation

$$1 + v = \frac{CD^4 E\varphi}{2LT} \tag{7}$$

whereby the RHS term is a dimensionless group.

For an arbitrary cross-section with a hollow of similar shape, the polar moment of area is $J = C(D_o^4 - D_i^4)$ such that

$$1 + v = \frac{CD_o^4 E\varphi}{2LT}\left[1 - \left(\frac{D_i}{D_o}\right)^4\right], \tag{8}$$

whereby a similar dimensionless group appears on the RHS. It can be seen for both cases that the effective Poisson's ratio of a rod consisting of an inner core of arbitrary cross-section and a similarly shaped outer shell undergoing torsion is a function of two dimensionless groups

$$v_{\mathrm{TOR}} = f\left(\frac{CD_o^4 E_n\varphi}{2LT}, \frac{D_i}{D_o}\right); \quad (n = 1, 2) \tag{9}$$

A benefit of expressing the effective torsional Poisson's ratio in terms of the characteristic dimension and a geometrical dimension is in its generic applicability such that a master curve can be plotted for representing a generalized rod cross-section under infinitesimal torsion, see Table 1. Another benefit is the identification of a dimensionless group, from which the effective Poisson's ratio of a compound rod can be inferred.

A rod consisting of an outer shell and an inner core with similar shape is a simplified case of a concentrically arranged rod. Hence the overall torsion is combined from both components while the angular twist is common

$$T = T_i + T_o = \frac{\varphi}{L}(G_i J_i + G_o J_o), \tag{10}$$

such that

Table 1 Generalization polar moment of area using characteristic dimension and a geometrical coefficient

Cross-sectional shape	Cross-sectional dimension	Coefficient of polar moment cross-section	Polar moment area for solid rod	Polar moment area for hollow rod
Arbitrary	Characteristic dimension, D	C	CD^4	$CD_o^4\left[1-\left(\frac{D_i}{D_o}\right)^4\right]$
Circular	Diameter, d	$\frac{\pi}{32}$	$\frac{\pi}{32}d^4$	$\frac{\pi}{32}d_o^4\left[1-\left(\frac{d_i}{d_o}\right)^4\right]$
Square	Side, a	$\frac{1}{6}$	$\frac{1}{6}a^4$	$\frac{1}{6}a_o^4\left[1-\left(\frac{a_i}{a_o}\right)^4\right]$
Equilateral triangle	Side, b	$\frac{\sqrt{3}}{48}$	$\frac{\sqrt{3}}{48}b^4$	$\frac{\sqrt{3}}{48}b_o^4\left[1-\left(\frac{b_i}{b_o}\right)^4\right]$

$$\frac{TL}{\varphi}=\frac{CD_i^4E_i}{2(1+\nu_i)}+\frac{C(D_o^4-D_i^4)E_o}{2(1+\nu_o)}. \tag{11}$$

To pave a way for comparison and illustration, normalization is imposed for both the inner core and outer shell materials. Normalizing the Young's modulus $E_i = E_o = E$, we obtain an expression for the inverse of the dimensionless group,

$$\frac{2TL}{CD_o^4E\varphi}=\frac{\left(\frac{D_i}{D_o}\right)^4}{1+\nu_i}+\frac{1-\left(\frac{D_i}{D_o}\right)^4}{1+\nu_o}. \tag{12}$$

On the basis of the effective torsional Poisson's ratio being functions of the identified dimensionless groups as described in Eq. 7, the effective Poisson's ratio under torsional load can be inferred as

$$1+\nu_{TOR}=\frac{CD_o^4E\varphi}{2LT} \tag{13}$$

such that substituting Eq. 12 into Eq. 13 gives

$$\nu_{TOR}=\frac{(1+\nu_o)(1+\nu_i)}{(1+\nu_o)\left(\frac{D_i}{D_o}\right)^4+(1+\nu_i)\left[1-\left(\frac{D_i}{D_o}\right)^4\right]}-1 \tag{14}$$

For comparison with the Poisson's ratio under axial loading, we have its corresponding effective Poisson's ratio

$$\nu_{AX}=\left(\frac{D_i}{D_o}\right)^2\nu_i+\left[1-\left(\frac{D_i}{D_o}\right)^2\right]\nu_o. \tag{15}$$

To illustrate the change in the overall auxeticity of a semi-auxetic rod, we consider a special category whereby the Poisson's ratio of the core and shell possess equal magnitude but opposite signs. Since the Poisson's ratio of an isotropic material is within the range $-1 \le \nu \le 0.5$, we select two cases: (i) auxetic core, in which the inner core Poisson's ratio is $\nu_i = -0.5$ and the outer shell Poisson's ratio is $\nu_o = 0.5$, and (ii) auxetic shell in which $\nu_i = 0.5$ and $\nu_o = -0.5$. See Fig. 2.

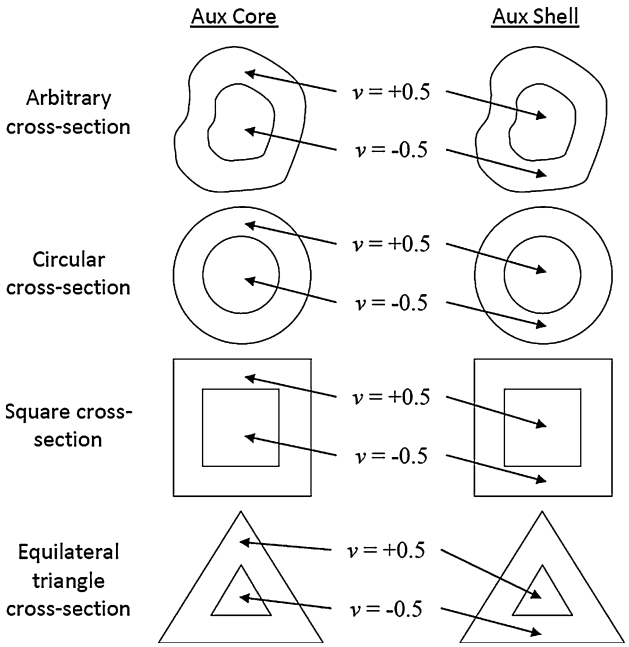

Fig. 2 The various semi-auxetic combined rods which can be represented by the arbitrary cross-section on the basis of Eq. 14

Auxetic core rod

For the special case of auxetic core rod, the effective Poisson's ratio under axial loading mode and torsional loading mode are

$$\nu_{AX}=\frac{1}{2}-\left(\frac{D_i}{D_o}\right)^2 \tag{16}$$

and

$$\nu_{TOR}=\frac{3}{6\left(\frac{D_i}{D_o}\right)^4+2\left[1-\left(\frac{D_i}{D_o}\right)^4\right]}-1, \tag{17}$$

respectively. Plots of the effective Poisson's ratios with reference to the inner-to-outer characteristic dimension ratio, (D_i/D_o), are shown in Fig. 3.

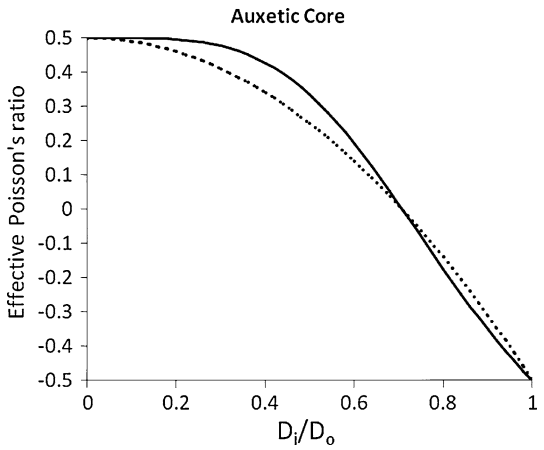

Fig. 3 The effective Poisson's ratio of a semi-auxetic rod with an auxetic core under axial load (*dashed curve*) and torsional load (*solid curve*)

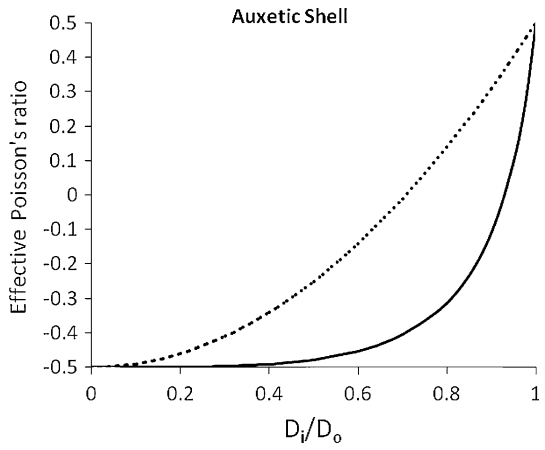

Fig. 4 The effective Poisson's ratio of a semi-auxetic rod with an auxetic shell under axial load (*dashed curve*) and torsional load (*solid curve*)

Perusal to this figure, as well as to Eqs. 16 and 17 show that such rods possess zero Poisson's ratio at $(D_i/D_o) = 0.5^{0.5}$ such that they exhibit an overall conventional behavior for $(D_i/D_o) < 0.5^{0.5}$ and overall auxetic behavior for $(D_i/D_o) > 0.5^{0.5}$. More strikingly, the effective Poisson's ratio is of higher magnitude when the rod undergoes torsion as compared to axial loading.

Auxetic shell rod

In the special case of auxetic shell, the effective Poisson's ratio for axial and torsional loading modes are

$$\nu_{AX} = -\frac{1}{2} + \left(\frac{D_i}{D_o}\right)^2 \tag{18}$$

and

$$\nu_{TOR} = \frac{3}{2\left(\frac{D_i}{D_o}\right)^4 + 6\left[1 - \left(\frac{D_i}{D_o}\right)^4\right]} - 1, \tag{19}$$

respectively. Variation of the effective Poisson's ratios with respect to the inner-to-outer characteristic dimension ratio, (D_i/D_o), are plotted in Fig. 4.

As in the previous section, the effective Poisson's ratio for axial loading is zero at $(D_i/D_o) = 0.5^{0.5}$. Unlike the previous case, the effective Poisson's ratio, under the influence of torsional load, is zero at $(D_i/D_o) = 0.75^{0.25}$. As a result the rod exhibits an overall auxetic behavior for $(D_i/D_o) < 0.5^{0.5}$ and an overall conventional behavior for $(D_i/D_o) > 0.75^{0.25}$ regardless of the loading mode. For the range $0.5^{0.5} < (D_i/D_o) < 0.75^{0.25}$, the rod exhibits a mixed behavior which is loading mode dependant, i.e., it behaves as a conventional rod when an axial load is imposed but as an auxetic rod during twisting.

Discussion

For the purpose of symmetry, the plots of effective Poisson's ratio of the combined rods in Figs. 3 and 4 are replotted against the inner-to-outer characteristic dimensions raised to the second and fourth powers, respectively, as depicted in Figs. 5 and 6.

The range of the inner-to-outer rod dimension that gives rise to different auxeticity levels, i.e.,

$$\left.\begin{array}{l} 0 < \nu_{AX} < \nu_{TOR};\ 0.0 < (D_i/D_o)^2 < 0.5 \\ \nu_{TOR} < \nu_{AX} < 0;\ 0.5 < (D_i/D_o)^2 < 1.0 \end{array}\right\} \Leftrightarrow \left\{\begin{array}{l} \nu_i \\ \nu_o \end{array}\right\} = \frac{1}{2}\left\{\begin{array}{l} -1 \\ +1 \end{array}\right\} \tag{20}$$

for the auxetic core and

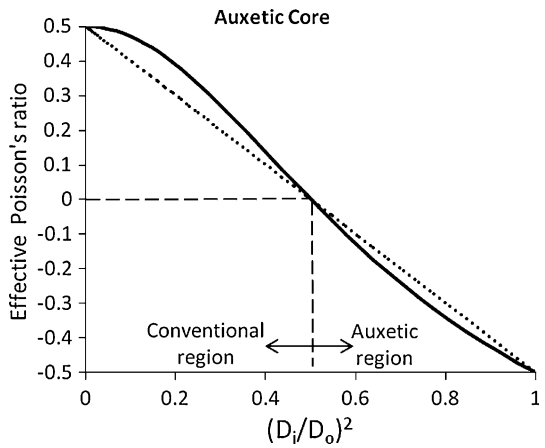

Fig. 5 A symmetric plot of the effective Poisson's ratio of a semi-auxetic rod with an auxetic core under axial load (*dashed curve*) and torsional load (*solid curve*)

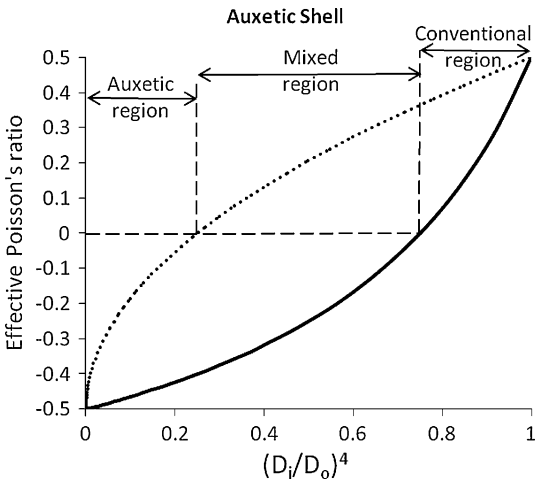

Fig. 6 A symmetric plot of the effective Poisson's ratio of a semi-auxetic rod with an auxetic shell under axial load (*dashed curve*) and torsional load (*solid curve*)

$$\left.\begin{array}{l} \nu_{TOR} < \nu_{AX} < 0;\ 0.00 < (D_i/D_o)^4 < 0.25 \\ \nu_{TOR} < 0 < \nu_{AX};\ 0.25 < (D_i/D_o)^4 < 0.75 \\ 0 < \nu_{TOR} < \nu_{AX};\ 0.75 < (D_i/D_o)^4 < 1.00 \end{array}\right\} \Leftrightarrow \left\{\begin{array}{l} \nu_i \\ \nu_o \end{array}\right\} = \frac{1}{2}\left\{\begin{array}{l} +1 \\ -1 \end{array}\right\} \quad (21)$$

for the auxetic shell may well be elucidated by the area property of the rod cross-section. In the case of auxetic shell, the higher auxeticity that is manifested during torsional loading mode as compared to axial loading mode is attributed to the greater influence of the outermost rod material. This results in a more negative effective Poisson's ratio during torsion than during axial loading for any value of (D_i/D_o). In the case of auxetic core, the lower auxeticity for torsional loading as compared to that of axial loading for a relatively small core is due to the strong influence of the conventional shell. As (D_i/D_o) increases, the overall auxeticity of the rod in the context of torsional loading catches up and exceeds the overall auxeticity in the context of axial loading.

Conclusions

An indirect way for describing the effective Poisson's ratio of a prismatic rod undergoing torsional loading has been proposed and applied for the case of a concentrically compound rod consisting of an inner core and outer shell of similar shape but opposite Poisson's ratio signs.

Within the category of whereby the core and shell possess equal Poisson's ratio magnitude, plotted results reveal different torsional loading auxeticity but equal axial loading auxeticity. For a concentric compound rod with auxetic core and conventional shell, the sign of the effective Poisson ratio under torsional loading follows that under axial loading, but with slightly greater magnitude. For a concentric compound rod with conventional core and auxetic shell, there is a range of relative volume fraction whereby the rod exhibits overall conventional and auxetic behavior under axial and torsional loading modes, respectively. This phenomenon has been elucidated herein from the standpoint of cross-sectional area properties of rods undergoing axial and torsional loading modes. Hence a compound rod with auxetic shell exhibits greater extent of loading mode-dependent auxeticity than that with auxetic core. The present results suggests the use of a compound rod with conventional core and auxetic shell as a smart structure that gives different response depending on the type of loading imposed on it.

References

1. Miller W, Smith CW, Mackenzie DS, Evans KE (2009) J Mater Sci 44:5441. doi:10.1007/s10853-009-3692-4
2. Lu QQ, Cheng XN, yang J, Sun XJ (2011) J Mater Sci 46:1253. doi:10.1007/s10853-010-4905-6
3. Peng J, Wu MM, Guo FL, Han SB, Liu YT, Chen DF, Zhao XH, Hu Z (2011) J Mater Sci 46:5160. doi:10.1007/s10853-011-5447-2
4. Srinivasan MV, Kannan P (2011) J Mater Sci 46:5029. doi:10.1007/s10853-011-5423-x
5. Popereka MYA, Balagurov VG (1969) Fiz Tverd Tela 11:3507
6. Milstein F, Huang K (1979) Phys Rev B 19:2030
7. Lakes R (1987) Science 235:1038
8. Lakes R (1987) Science 238:551
9. Wojciechowski KW (1989) Phys Lett A 137:60
10. Wojciechowski KW, Branka AC (1989) Phys Rev A 40:7222
11. Caddock BD, Evans KE (1989) J Phys D 22:1877
12. Evans KE, Caddock BD (1989) J Phys D 22:1883
13. Bianchi M, Scarpa F, Banse M, Smith CW (2011) Acta Mater 59:686
14. Gaspar N, Smith CW, Alderson A, Grima JN, Evans KE (2011) J Mater Sci 46:372. doi:10.1007/s10853-010-4846-0
15. Grima JN, Manicaro E, Attard D (2011) Proc R Soc A 467:439
16. Taylor CM, Smith CW, Miller W, Evans KE (2011) Int J Solids Struct 48:1330
17. Lim TC, Acharya UR (2009) J Mater Sci 44:4491. doi:10.1007/s10853-009-3657-7
18. Bianchi M, Scarpa F, Smith CW, Whittell GR (2010) J Mater Sci 45:341. doi:10.1007/s10853-009-3940-7
19. Milton GW (1992) J Mech Phys Solids 40:1105
20. Wei G, Edwards SF (1998) Physica A 258:5
21. Wei G, Edwards SF (1998) Phys Rev E 58:6173
22. Donoghue JP, Alderson KL, Evans KE (2009) Phys Status Solidi B 246:2011
23. Evans KE, Donoghue JP, Alderson KL (2004) J Compos Mater 38:95
24. Alderson KL, Simkins VR, Coenen VL, Davies PJ, Alderson A, Evans KE (2005) Phys Status Solidi B 242:509
25. Simkins VR, Alderson A, Davies PJ, Alderson KL (2005) J Mater Sci 40:4355. doi:10.1007/s10853-005-2829-3
26. Coenen VL, Alderson KL (2011) Phys Status Solidi B 248:66

27. Jayanty S, Crowe J, Berhan L (2011) Phys Status Solidi B 248:73
28. Donescu S, Chiroiu V, Munteanu L (2009) Mech Res Commun 36:294
29. Kocer C, McKenzie DR, Bilek MM (2009) Mater Sci Eng A 505:111
30. Lim TC (2009) Eur J Mech A 28:752
31. Chirima GT, Zied KM, Ravirala N, Alderson KL, Alderson A (2009) Phys Status Solidi B 246:2072
32. Lim TC, Rajendra Acharya U (2011) Phys Status Solidi B 248:60
33. Lim TC (2010) J Eng Mech 136:1176
34. Lim TC, Rajendra Acharya U (2010) J Reinf Plast Compos 29:1441
35. Lim TC (2002) J Mater Sci Lett 21:1899
36. Gatt R, Attard D, Grima JN (2009) Scr Mater 60:65
37. Scarpa F, Tomlinson G (1998) In: Proceedings of the 23rd International Conference on Noise and Vibration Engineering ISMA 803-807, Leuven
38. Ruzzene M, Scarpa F (2001) Proc SPIE 4331:443
39. Scarpa F, Ruzzene M, Mazzarella L, Tsopelas P (2002) Proc SPIE 4697:176
40. Whitty JPM, Alderson A, Myler P, Kandola B (2003) Composites A 34:525
41. Lim TC (2007) Phys Status Solidi B 244:910
42. Uzer G, Ding Y, Chiang FP (2007) In: Proceedings of the SEM Annual Conference and Exposition on Experimental and Applied Mechanics, vol 2, Springfield
43. Wen J, Wen X, Yu D (2008) In: Proceedings of the ASME International Design Engineering Technical Conferences and Computers and Information Engineering Conference DETC2007, Part A, Las Vegas
44. Michelis P, Spitas V (2010) Compos Sci Technol 70:1064
45. Miller W, Smith CW, Evans KE (2011) Compos Struct 93:1072
46. Khurram Wadee M, Ahmer Wadee M, Bassom AP (2007) J Mech Phys Solids 55:1086
47. Scarpa F, Smith CW, Ruzzene M, Wadee MK (2008) Phys Status Solidi B 245:584
48. Kolat P, Maruszewski BT, Tretiakov KV, Wojciechowski KW (2011) Phys Status Solidi B 248:148